Hyperpolarizabilities of hydrogenlike atoms in Debye and dense quantum plasmas

Yu Ying He,[1] Zhi Ling Zhou,[1] Li Guang Jiao,[1,2,3,*] Aihua Liu,[4,†] H. E. Montgomery, Jr.,[5] and Yew Kam Ho[6]

[1]*College of Physics, Jilin University, Changchun 130012, People's Republic of China*
[2]*Helmholtz-Institut Jena, D-07743 Jena, Germany*
[3]*Theoretisch-Physikalisches Institut, Friedrich-Schiller-Universität Jena, D-07743 Jena, Germany*
[4]*Institute of Atomic and Molecular Physics, Jilin University, Changchun 130012, People's Republic of China*
[5]*Chemistry Program, Centre College, Danville, Kentucky 40422, USA*
[6]*Institute of Atomic and Molecular Sciences, Academia Sinica, Taipei 10617, Taiwan*

(Received 23 December 2022; accepted 22 March 2023; published 18 April 2023)

The hyperpolarizabilities of the hydrogenlike atoms in Debye and dense quantum plasmas are calculated using the sum-over-states formalism based on the generalized pseudospectral method. The Debye-Hückel and exponential-cosine screened Coulomb potentials are employed to model the screening effects in, respectively, Debye and dense quantum plasmas. Our numerical calculation demonstrates that the present method shows exponential convergence in calculating the hyperpolarizabilities of one-electron systems and the obtained results significantly improve previous predictions in the strong screening environment. The asymptotic behavior of hyperpolarizability near the system bound-continuum limit is investigated and the results for some low-lying excited states are reported. By comparing the fourth-order corrected energies in terms of hyperpolarizability with the resonance energies using the complex-scaling method, we empirically conclude that the applicability of hyperpolarizability in perturbatively estimating the system energy in Debye plasmas lies in the range of $[0, F_{\max}/2]$, where $F_{\max}$ refers to the maximum electric field strength at which the fourth-order energy correction is equal to the second-order term.

DOI: 10.1103/PhysRevE.107.045201

I. INTRODUCTION

Investigation of the plasma screening effect on atomic structural properties and scattering dynamics has attracted considerable interest in the past decades due to its importance in diagnosing plasma parameters and understanding the elementary processes in plasmas [1–8]. The hyperpolarizability of an atom affected by plasma screening has become the focus of study in recent years [9–16]. Such a quantity is intimately related to the third-order nonlinear optical processes of atoms in external electric fields, such as the third-harmonic generation, the dc Kerr effect, electric-field-induced second-harmonic generation, and the degenerate four-wave mixing [17,18]. The static hyperpolarizability can be understood as the origin of the fourth-order energy correction when the atom is placed in a weak static electric field and the poles of frequency-dependent (dynamic) hyperpolarizability are directly related to the two-photon excitation energies of the system. For the free H atom, the static hyperpolarizability is known exactly [19,20] and the dynamic hyperpolarizability has also been obtained with very high accuracy [17]. However, the variation of these quantities even for the simplest H atom under plasma screenings has far from been established.

In this work, we focus on two model plasmas [21], i.e., the weakly coupled classical (Debye) and the dense quantum plasmas. The weakly coupled classical plasmas, which generally possess high temperatures and low densities, are usually modeled by the Debye-Hückel [22] or static screened Coulomb potential (SCP), $V(r) = \frac{Ze^2}{r}e^{-\lambda r}$, where $\lambda = 1/D$ is the screening parameter and $D = \sqrt{k_B T_e/(4\pi n_e)}$ is the Debye length [1]. For atomic or ionic targets embedded in these plasmas, the electron-nucleus and interelectronic Coulomb interactions are commonly replaced by the statically averaged SCPs (see Ref. [8] and references therein). In the extreme of opposite conditions, i.e., the strongly coupled quantum plasmas which are characterized by low temperatures and high densities, the quantum mechanical effects are nonnegligible in modeling the average interaction between charged particles because the de Broglie wavelength of the test charged particles may be comparable to the Debye length of plasmas. In this situation, the modified Debye-Hückel or exponential cosine screened Coulomb potential (ECSCP), $V(r) = \frac{Ze^2}{r}e^{-\lambda r}\cos(\lambda r)$, was developed by Shukla and Eliasson [23–25] and then was extensively employed in investigating various atomic properties in dense quantum plasmas (see Ref. [26] and references therein). The screening parameter, however, reads $\lambda = k_q/\sqrt{2}$ where $k_q = \sqrt{2m_e\omega_{pe}/\hbar}$ represents the electron quantum wave number in association with the electron plasma frequency ω_{pe} [23]. For convenience, we will use SCP and ECSCP to indicate, respectively, the Debye and dense quantum plasmas, and for the sake of generalization, we use a single screening parameter λ in both SCP and ECSCP by ignoring its explicit dependence on plasma parameters [21].

*lgjiao@jlu.edu.cn
†aihualiu@jlu.edu.cn

The first calculation of the hyperpolarizability of H atom in Debye plasmas initiates from Saha *et al.* [9], where the variational perturbation method based on Slater-type orbitals is employed to obtain the hyperpolarizability over a wide range of screening parameters. A significant enhancement of the hyperpolarizability at large screening parameters was observed. The dynamic hyperpolarizability and two-photon excitations of H atom in Debye plasmas were investigated by Bhattacharyya *et al.* [10] using time-dependent variational perturbation theory. In a subsequent work [11], these authors extended their calculations to dense quantum plasmas and compared the variation of hyperpolarizability in these two different screening conditions. The same computational method was recently employed by Chaudhuri *et al.* [12] in which they investigated the two-photon transition energies and probabilities of the H atom in both Debye and dense quantum plasmas. We also note that the hyperpolarizabilities for some multielectron atoms in different plasmas are available in the literature. For example, the hyperpolarizabilities of two-electron atoms under spherically confined Debye plasmas, strongly coupled plasmas, and dense quantum plasmas were obtained by Sen *et al.* [13,14] and Chaudhuri *et al.* [15], where the variational perturbation theory within the coupled Hartree-Fock scheme has been adopted to take into account partial electron correlation effects. The influence of Debye plasmas on the hyperpolarizability of the lithium atom was surveyed by Kang *et al.* [16] utilizing a linear variation method based on B-spline basis functions. In their research, a one-electron model potential was employed to simplify the three-electron atom and, furthermore, the plasma screening effect was introduced empirically on the model potential. In what follows we will focus on the H-like atoms, which excludes the complexities due to electron correlation, and primarily pay our attention to the plasma screening effect on the hyperpolarizability.

In this work, we employ the sum-over-states formalism to calculate the hyperpolarizabilities of H-like atoms in both the ground and excited states embedded in Debye and dense quantum plasmas. The generalized pseudospectral (GPS) method [27–29] in discrete variable representation is adopted to efficiently and accurately produce the system eigenenergies and wave functions. The combination of these two techniques enables us to obtain accurate hyperpolarizability over the entire range of screening parameters where the system is still bound, and opens the possibility of analyzing the intriguing phenomena of the system in extreme conditions introduced by plasmas. This paper is organized as follows. Section II details the theoretical method employed in this work. The results and discussion are given in Sec. III, which includes the convergence test of our numerical calculations, the comparison with previous predictions, the variation and asymptotic behavior of hyperpolarizability in both the ground and excited states, and a discussion on the applicability of the hyperpolarizability. We summarize the present work in Sec. IV. Atomic units (a.u.) are used throughout this paper unless otherwise mentioned.

II. THEORETICAL METHOD

The time-independent Schrödinger equation for the one-electron atom in the presence of an external static electric field can be formally written as

$$H|\psi_k\rangle = E_k|\psi_k\rangle, \tag{1}$$

where the full Hamiltonian of the system consists of two parts, i.e.,

$$H = H^{(0)} + FH'. \tag{2}$$

$H^{(0)}$ is the unperturbed Hamiltonian of the one-electron atom in the form

$$H^{(0)} = -\frac{1}{2}\frac{d^2}{dr^2} + \frac{l(l+1)}{2r^2} + V(r), \tag{3}$$

where the effective potential in the plasma environment reads

$$V(r) = \begin{cases} -\frac{Z}{r}e^{-\lambda r} & \text{(SCP)}, \\ -\frac{Z}{r}e^{-\lambda r}\cos(\lambda r) & \text{(ECSCP)}. \end{cases} \tag{4}$$

It is worth noting that, when $\lambda = 0$, both SCP and ECSCP reduce to the Coulomb potential in free H-like ions. In Eq. (2), F represents the strength of the homogeneous static electric field, and H' refers to the strength-independent interaction between the atom and external electric field, which in the dipole approximation, is given by

$$H' = -r\cos\theta. \tag{5}$$

Here we chose the electric field F in the z direction and, correspondingly, θ is the polar angle of the electron.

When the electric field is relatively weak so that the field-atom interaction can be treated as a perturbation to the Coulomb interaction, the system eigenenergies and wave functions can be expanded as power series in terms of the field strength F [30],

$$E_k = E_k^{(0)} + FE_k^{(1)} + F^2E_k^{(2)} + F^3E_k^{(3)} + F^4E_k^{(4)} + \ldots, \tag{6}$$

$$|\psi_k\rangle = |\psi_k^{(0)}\rangle + F|\psi_k^{(1)}\rangle + F^2|\psi_k^{(2)}\rangle + F^3|\psi_k^{(3)}\rangle + F^4|\psi_k^{(4)}\rangle + \ldots, \tag{7}$$

where the lowest-order energies and wave functions satisfy the Schrödinger equation of the unperturbed Hamiltonian $H^{(0)}$

$$H^{(0)}|\psi_k^{(0)}\rangle = E_k^{(0)}|\psi_k^{(0)}\rangle, \tag{8}$$

and the wave functions form a complete set of orthonormal eigenfunctions

$$\langle\psi_{k'}^{(0)}|\psi_k^{(0)}\rangle = \delta_{kk'}. \tag{9}$$

Following the standard perturbation theory of quantum mechanics and considering that the dipole interaction shown in Eq. (5) is in odd parity, it is readily obtained that all odd-order energy corrections vanish and only even-order terms survive. The static dipole polarizability (α) and hyperpolarizability (γ) of the one-electron system are then defined through the second- and fourth-order energy corrections [31], respectively, by

$$\alpha = -2E_k^{(2)}, \tag{10}$$

and

$$\gamma = -24E_k^{(4)}. \tag{11}$$

In the sum-over-states formalism [18], the second- and fourth-order energy corrections can be formally written as

$$E_k^{(2)} = \sum_{n\in p}{}' \frac{|H'_{n,k}|^2}{E_k^{(0)} - E_n^{(0)}}, \tag{12}$$

and

$$E_k^{(4)} = \sum_{j\in p}{}' \left(\sum_{i\in s,d}{}' \sum_{n\in p}{}' \frac{H'_{k,j}H'_{j,i}H'_{i,n}H'_{n,k}}{\left(E_k^{(0)} - E_j^{(0)}\right)\left(E_k^{(0)} - E_i^{(0)}\right)\left(E_k^{(0)} - E_n^{(0)}\right)} - \sum_{n\in p}{}' \frac{|H'_{j,k}|^2 |H'_{n,k}|^2}{\left(E_k^{(0)} - E_j^{(0)}\right)^2 \left(E_k^{(0)} - E_n^{(0)}\right)} \right), \tag{13}$$

where $H'_{j,i}$ refers to the dipole transition matrix element from the initial $|i\rangle$ to the final $|j\rangle$ states

$$H'_{j,i} = \langle \psi_j^{(0)} | H' | \psi_i^{(0)} \rangle. \tag{14}$$

In this work, we are interested in the polarizabilities for the s-wave states of the H-like atoms. Therefore, in both Eqs. (12) and (13), the indexes n and j run over all p-wave states and the index i runs over all s- and d-wave states. This is due to the fact that the dipole transition only permits the angular momentum selection rule of $\Delta l = \pm 1$. It is then obvious that the dipole polarizability of atoms with s-wave initial state involves $s \to p$ one-photon transitions and the dipole hyperpolarizability involves both $s \to p \to s$ and $s \to p \to d$ two-photon transitions. It is also worth noting that the primes in the summations over n, i, and j in Eqs. (12) and (13) indicate the omission of any intermediate states that are degenerate with the initial state $|\psi_k^{(0)}\rangle$.

From the above discussion it is clear that the transition matrices in Eqs. (12) and (13) involve only $s \to p$ and $p \to d$ dipole transitions, and the magnetic quantum numbers for all final states are restricted to zeros, considering the initial state in s-wave symmetry. The transition matrix of Eq. (14) thus reduces to

$$H'_{j,i} = \langle r \rangle_{n_i l_i}^{n_j l_j} \sqrt{(2l_i+1)(2l_j+1)} \begin{Bmatrix} l_j & 1 & l_i \\ 0 & 0 & 0 \end{Bmatrix}^2, \tag{15}$$

where the radial component reads

$$\langle r \rangle_{n_i l_i}^{n_j l_j} = \int_0^\infty R_{n_j l_j}(r) r R_{n_i l_i}(r) r^2 dr, \tag{16}$$

in which $R_{n_i l_i}(r)$ and $R_{n_j l_j}(r)$ are the radial parts of the initial and final state wave functions, respectively. An accurate calculation of polarizability and hyperpolarizability requires (i) the complete spectrum of the unperturbed system including both bound and (pseudo) continuum states, and (ii) the accurate computation of each radial transition matrix element.

In this work, we employ the generalized pseudospectral (GPS) method to accomplish this task. The implementation details of the GPS method are available elsewhere and interested readers are referred to Refs. [27–29] for details. As a numerical method formulated in discrete variable representation, the GPS method has shown its high flexibility and fast convergence in calculating the bound-state energies and wave functions for one-electron systems [29]. After mapping the semi-infinite range of $r \in [0, \infty]$ onto $x \in [-1, 1]$, discretizing the radial variable x based on the Legendre-Gauss-Lobatto quadrature, and solving the standard eigenvalue problem for the transformed radial Schrödinger equation, the radial component of the transition matrix is expressed as

$$\langle r \rangle_{n_i l_i}^{n_j l_j} = \sum_{k=0}^{N} f(x_k) \phi_{n_j l_j}(x_k) \phi_{n_i l_i}(x_k) \omega_k, \tag{17}$$

where $f(x)$ is the mapping function in the form

$$r = f(x) = L \frac{1+x}{1-x}, \tag{18}$$

$\phi_{nl}(x)$ is the transformed radial wave function defined by

$$\frac{\phi_{nl}(x)}{\sqrt{f'(x)}} = r R_{nl}(r), \tag{19}$$

and x_k and ω_k are, respectively, abscissas and weights of the Legendre-Gauss-Lobatto quadrature [32]. It is worth noting that Eq. (17) is derived on the assumption that the same mapping function $f(x)$ and same total number of mesh points N are employed for both the initial and final states. For a more general expression where the initial and final states are obtained with different mapping functions at different mesh points, interested readers are referred to Eq. (30) of Ref. [33]. For convenience Eq. (17) is used throughout the present calculations, and in doing so, we only need to gradually increase N to achieve converged numerical results.

In our previous work [26], we derived that there exists a Z-scaling law for the multipole polarizabilities of H-like ions with respect to the nuclear charge

$$\alpha^{(k)}(\delta) = Z^{2(k+1)} \alpha^{(k)}(Z, \lambda), \tag{20}$$

where k refers to the order of multipole expansion of the electric radiative transition operator and

$$\delta = \frac{\lambda}{Z}. \tag{21}$$

For the dipole polarizability it is readily obtained that $\alpha(\delta) = Z^4 \alpha(Z, \lambda)$ [here we delete the superscript (1) by focusing in this work only on the dipole transition]. Following the same procedure, we obtain the Z-scaling law for dipole hyperpolarizability in the form

$$\gamma(\delta) = Z^{10} \gamma(Z, \lambda). \tag{22}$$

In our following work, we will focus on the neutral H atom, but keep in mind that the polarization quantities for H-like ions and any other two-body systems can be gained straightforwardly.

III. RESULTS AND DISCUSSION

A. Convergence of calculation

To test the convergence and accuracy of the present numerical calculations based on the GPS method, we provide in Table I the ground-state energy, dipole polarizability, and hyperpolarizability of the H atom under SCP at some selected values of screening parameter. The total number of mesh points N is gradually increased to ensure that all reported numerical results converge to the last digit shown in the table. For the ground state of a free H atom where

TABLE I. Convergence of the ground-state energy ($E^{(0)}$), dipole polarizability (α), and hyperpolarizability (γ) for the H atom under SCP at $\lambda = 0$, 0.1, 1.0, and 1.15. $L = 10$ in the mapping function is used throughout the calculations. Numbers in parentheses represent powers of ten. The converged results for $E^{(0)}$, α, and γ are indicated by **bold numbers**.

λ	N	$-E^{(0)}$	α	γ
0	20	**5.000000000000**6908020(−1)	**4.50000000**59861588371	**1.3331250**1858856071 70(3)
	30	**5.000000000000000000**35(−1)	**4.500000000000000**164156	**1.33312499999**89915239(3)
	40	**5.000000000000000000000**(−1)	**4.500000000000000000000**	**1.33312500000000000**246(3)
	50	**5.000000000000000000000**(−1)	**4.500000000000000000000**	**1.33312500000000000000**(3)
0.1	20	**4.07058030613**32005914(−1)	**4.6997774**736678969249	**1.567590**1603037754557(3)
	30	**4.0705803061340315671**(−1)	**4.699777471480**3966172	**1.56759007470**33090710(3)
	40	**4.0705803061340315675**(−1)	**4.6997774714803895**29	**1.5675900747027283**676(3)
	50	**4.0705803061340315675**(−1)	**4.6997774714803895330**	**1.56759007470272837 10**(3)
1.0	40	**1.028578999001**7700458(−2)	**7.834765746**4167589943(2)	**6.27844031**58356940078(9)
	60	**1.0285789990017696805**(−2)	**7.8347657464284417**354(2)	**6.2784403196**732991438(9)
	80	**1.0285789990017696805**(−2)	**7.8347657464284419499**(2)	**6.27844031967293666**947(9)
	100	**1.0285789990017696805**(−2)	**7.8347657464284419499**(2)	**6.27844031967293666662**(9)
1.15	100	**4.5588902135595778**646(−4)	**3.176138469270**7120940(5)	**3.00264131210**47833615(16)
	120	**4.55889021355957785 68**(−4)	**3.176138469270782**0913(5)	**3.00264131211**32694321(16)
	140	**4.55889021355957785 68**(−4)	**3.176138469270781 4**781(5)	**3.00264131211133**278515(16)
	160	**4.55889021355957785 68**(−4)	**3.176138469270781 4813**(5)	**3.00264131211332 9**3239(16)
	180	**4.55889021355957785 68**(−4)	**3.176138469270781 4813**(5)	**3.00264131211332925**15(16)
	200	**4.55889021355957785 68**(−4)	**3.176138469270781 4813**(5)	**3.00264131211332925 27**(16)

there exist exact results for energy ($E = -0.5$), dipole polarizability ($\alpha = 4.5$), and hyperpolarizability ($\gamma = 1333.125$), we demonstrate in Fig. 1 the relative errors of the numerical calculations defined by

$$\delta^O = \left| \frac{\langle O \rangle_{\text{num}} - \langle O \rangle_{\text{exact}}}{\langle O \rangle_{\text{exact}}} \right|. \tag{23}$$

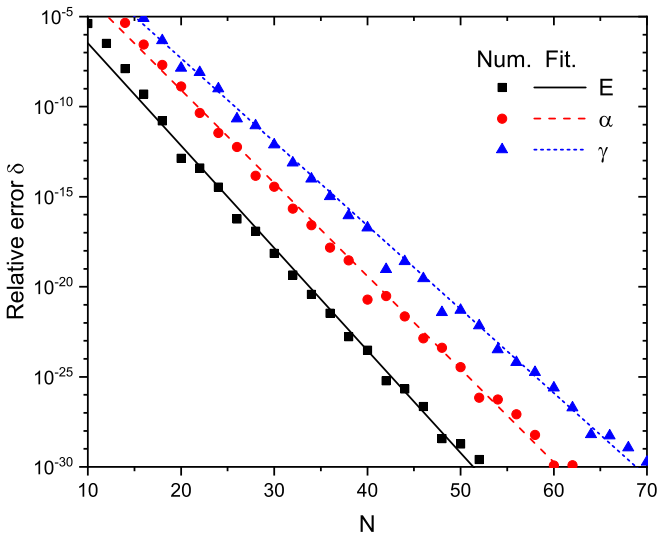

FIG. 1. Relative errors of the ground-state energy, dipole polarizability, and hyperpolarizability for the free H atom with increasing the number of mesh points N. The exact value of energy is $E = -0.5$. Exact dipole polarizability and hyperpolarizability are 4.5 and 1333.125, respectively. Dots represent the present GPS numerical calculations and lines refer to the fittings based on power functions of Eqs. (24) to (26).

It is observed that the GPS method possesses fast, exponential convergence for all the three quantities as functions of N. The exponential fittings of the numerical results yield

$$\delta^E(N) \propto e^{-1.31N}, \tag{24}$$

$$\delta^\alpha(N) \propto e^{-1.19N}, \tag{25}$$

$$\delta^\gamma(N) \propto e^{-1.07N}. \tag{26}$$

The system energy shows the most rapid convergence, which is due to the fact that its numerical accuracy simply is the quadratic order of the accuracy of system wave functions. The accuracy of dipole polarizability and hyperpolarizability are related to the fourth and eighth powers of the accuracy of system wave functions, respectively. Therefore, the convergence rate for polarizability is relatively slower than that for energy and the convergence for hyperpolarizability is slowest.

The ground-state energy, polarizability, and hyperpolarizability for the screened H atom in Debye plasmas for $\lambda = 0.1$, 1.0, and 1.15 are displayed in the lower part of Table I. The convergence rates for all the three quantities become slower at larger values of screening parameter, so one generally needs more mesh points to achieve a similar accuracy. This is because, as λ increases, the attractive screened Coulomb interaction becomes weaker and the electron probability density is distributed further away from the nucleus (e.g., the mean value of radius for the ground state of H atom is 1.5133, 4.3667, and 17.4465 for $\lambda = 0.1$, 1.0, and 1.15, respectively). Therefore, in a stronger screening environment a larger number of mesh points is necessary for discretizing the system wave function in the configuration space. Even so, exponential convergence is still observed in all numerical calculations. The fast convergence shown in Table I indicates that the GPS method is highly efficient and accurate in predicting the hyperpolarizabilities of one-electron systems in a plasma screening environment.

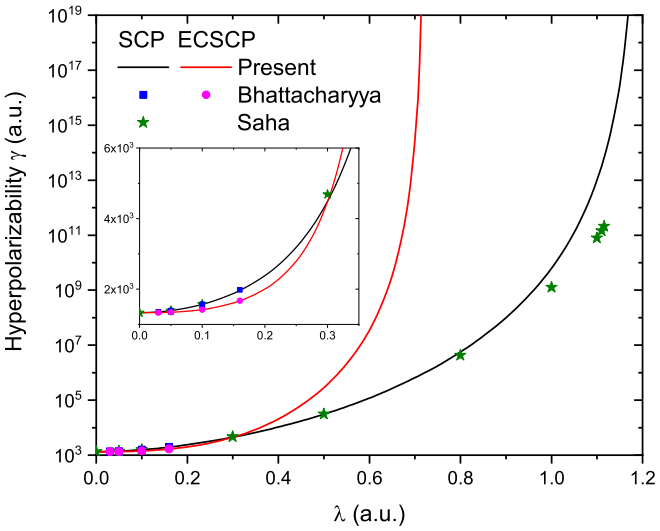

FIG. 2. Comparison of the hyperpolarizability for the ground state of H atom under SCP and ECSCP with the previous calculations of Saha *et al.* [9] and Bhattacharyya *et al.* [11]. The inset magnifies the comparison at small values of screening parameter and indicates the crossover phenomenon between the hyperpolarizabilities for SCP and ECSCP.

B. Ground state of the H atom under SCP and ECSCP

The hyperpolarizabilities for the ground state of the H atom under SCP and ECSCP are shown in Table II, together with the comparison with previous calculations of Saha *et al.* [9] and Bhattacharyya *et al.* [11]. The present calculations are performed by using $N = 300$ and $L = 50$, and the results shown in Table II are converged to their last reported digit. It has been well established that the critical screening parameters for the ground state of H atom in SCP and ECSCP are $\lambda_c = 1.190612421\ldots$ and $0.720524085\ldots$, respectively, beyond which the ground state ceases to exist [34,35]. When the screening parameter approaches a corresponding critical value, the bound-state energy approaches zero and the electron density distribution extends to an infinite region. As a result, both the dipole polarizability and hyperpolarizability are expected to be infinitely large. As is shown in Table II, the hyperpolarizabilities at $\lambda = 1.19$ for SCP and $\lambda = 0.72$ for ECSCP are 31 and 27 orders of magnitude greater than for $\lambda = 0$. These large values may become less useful in practical applications, but they give good evidence about the extremely diffuse character of the system wave function and further reveal the high stability of the present numerical method in extreme situations.

The comparisons of the present results with previous predictions of Saha *et al.* [9] and Bhattacharyya *et al.* [11] shown in Table II are also depicted in Fig. 2 for a clear view. In both of those two works, variational perturbation theory was employed to calculate the static dipole hyperpolarizability with the ground and perturbed wave functions represented by linear combinations of Slater-type orbitals. In the first work [9], the authors performed numerical calculations in SCP for screening parameters up to $\lambda = 1.1158$, which is very close to the critical screening parameter of the ground state. However, the difference between their results and the present calcu-

TABLE II. Hyperpolarizabilities for the ground state of H atom under SCP and ECSCP at some selected values of screening parameter λ. Numbers in parentheses represent powers of ten.

λ	γ^{SCP}	λ	γ^{ECSCP}
0	1.33312500000000(3)	0	1.33312500000000(3)
	1.333123(3)[a]		
0.01	1.33563563156775(3)	0.01	1.33323223570712(3)
0.02	1.34299629622742(3)	0.02	1.33395777840433(3)
0.03	1.35501552947499(3)	0.03	1.33585521958968(3)
	1.3554453(3)[b]		1.3359058(3)[b]
0.05	1.39263656835205(3)	0.05	1.34509124298012(3)
	1.3938(3)[a]		
	1.3938411(3)[b]		1.3453024(3)[b]
0.10	1.56759007470273(3)	0.10	1.41910847190232(3)
	1.5730(3)[a]		
	1.5730573(3)[b]		1.4205996(3)[b]
0.15	1.878662814144449(3)	0.15	1.60911767261550(3)
0.16	1.961407825811178(3)	0.16	1.66744774418353(3)
	1.9807084(3)[b]		1.6745049(3)[b]
0.20	2.381997944405400(3)	0.20	2.00164861275670(3)
0.25	3.185581190776900(3)	0.25	2.79101133303770(3)
0.29	4.174174433441960(3)	0.29	4.024607586261960(3)
0.30	4.489509242288380(3)	0.30	4.481620741472950(3)
	4.6876(3)[a]		
0.31	4.838907310068620(3)	0.31	5.025640560118400(3)
0.35	6.671999487136750(3)	0.35	8.580733267178760(3)
0.40	1.047590709263140(4)	0.40	2.045946414021940(4)
0.45	1.743150810361020(4)	0.45	6.416076804039980(4)
0.50	3.086916433219660(4)	0.50	2.864273416443800(5)
	3.1160(4)[a]		
0.55	5.850374363691920(4)	0.55	2.103930519207490(6)
0.60	1.195263403225760(5)	0.60	3.521280361730990(7)
0.65	2.657605509034780(5)	0.65	3.400187337299420(9)
0.70	6.512483192187690(5)	0.70	2.775033864344710(14)
0.75	1.789250137329430(6)	0.71	1.710169300184730(17)
0.80	5.644478210925490(6)	0.715	9.395570713522140(19)
	4.2501(6)[a]		
0.85	2.115949089132620(7)	0.718	2.175078376041870(23)
0.90	9.923296213976100(7)	0.719	3.279709038985500(25)
0.95	6.316881524651270(8)	0.72	1.377808775994540(30)
1.00	6.278440319672940(9)		
	1.2727(9)[a]		
1.10	1.006791775598350(13)		
	7.9187(10)[a]		
1.11	3.225387127829450(13)		
	1.4412(11)[a]		
1.1157	6.696021409158480(13)		
	2.0947(11)[a]		
1.1158	6.785725830692640(13)		
	2.1090(11)[a]		
1.12	1.206734278724500(14)		
1.14	3.338860421658550(15)		
1.15	3.002641312113330(16)		
1.16	5.047422785063850(17)		
1.17	2.622652724619580(19)		
1.18	1.994800856658710(22)		
1.185	1.162944791735490(25)		
1.189	3.030370383562390(30)		
1.19	4.848244741736340(34)		

[a]Saha *et al.* [9].
[b]Bhattacharyya *et al.* [11].

lations increases significantly as λ increases. For instance, for $\lambda < 0.1$ they predicted slightly larger values of hyperpolarizability than our calculations, while for $\lambda > 1.1$ their results are two orders of magnitude smaller than ours. This discrepancy is probably attributable to the insufficient number of Slater-type orbitals used in constructing the perturbed wave functions. In the subsequent work of Bhattacharyya *et al.* [11], the authors focused on the variation of static and dynamic hyperpolarizabilities at relatively small screening parameters ($\lambda \leqslant 0.16$). Their numerical results generally reproduce the predictions of Saha *et al.* [9] in SCP, and are systematically larger than our calculations in both SCP and ECSCP. Another calculation of the hyperpolarizabilities of H-like atoms in SCP comes from the most recent work of Bhatia and Drachman [36] in the sum-over-states formalism, where pseudostates for s, p, d, and f states are also constructed by utilizing the Slater-type orbitals. However, those authors defined two physical quantities named by the third-order polarizability and the fourth-order hyperpolarizability (see Eqs. (7) and (8) in Refs. [36,37] for their definitions), which use similar but different formalism compared to the second and first terms on the right-hand side of our Eq. (13). Unfortunately, we are unable to make a direct comparison of their numerical results to the present calculations.

The comparison between SCP and ECSCP reveals another interesting phenomenon: although the ECSCP manifests a stronger screening effect on the Coulomb potential than SCP, its hyperpolarizability is smaller at relatively small screening parameters. The crossover point is located at about $\lambda = 0.30$, after which the increasing speed of ECSCP is much faster than that of SCP. A similar phenomenon was observed in the dipole polarizability where the result for ECSCP goes across that for SCP at about $\lambda = 0.368$ [38]. Therefore, even though the zeroth-order energy of the system in the electric field strictly satisfies the inequality $E^{(0)}_{\mathrm{SCP}} \leqslant E^{(0)}_{\mathrm{ECSCP}}$, which is established from the comparison theorem of quantum mechanics [39], one must be careful about the comparison of total energy between different potentials due to the diverse contributions from high-order energy corrections.

C. Asymptotic behavior of hyperpolarizability

In addition to the high-precision numerical values of hyperpolarizability in the range of screening parameters where the bound state survives, we are also interested in its asymptotic behavior near the system bound-continuum limit, i.e., at λ near λ_c. In our previous work [26], we approximately derived and numerically verified that, when $\lambda \to \lambda_c$, the multipole polarizabilities for the s-wave states of one-electron systems obey power laws as a function of $\lambda_c - \lambda$,

$$\alpha^{(k)}(\lambda) \propto (\lambda_c - \lambda)^{-2(k+1)}. \tag{27}$$

For the dipole polarizability, i.e., $k = 1$, it readily has $\alpha(\lambda) \propto (\lambda_c - \lambda)^{-4}$ [the superscript (1) is omitted].

The asymptotic behavior for the dipole polarizability can be easily understood from the approximate formulas such as the Kirkwood [40], Buckingham [41], Unsöld [42], and Dalgarno and Lewis [43] expressions (see Eqs. (19) to (23) in Ref. [26] for their explicit forms), where the first two are lower bounds to the exact dipole polarizability for a spherical s-wave state and the second two are upper bounds for the ground state [44]. The asymptotic formula then can be obtained by utilizing the critical behaviors of the s-wave state energies

$$E_{ns}(\lambda) \propto (\lambda_c - \lambda)^2, \tag{28}$$

and corresponding radial expectation values

$$\langle r^k \rangle_{ns}(\lambda) \propto (\lambda_c - \lambda)^{-k}, \tag{29}$$

with the further assumptions that Unsöld [42] and Dalgarno and Lewis [43] approximations are still valid and the eigenenergy of the $2p$ state at screening parameters near $\lambda_c(1s)$ (more precisely, the lowest p-wave continuum state) is zero.

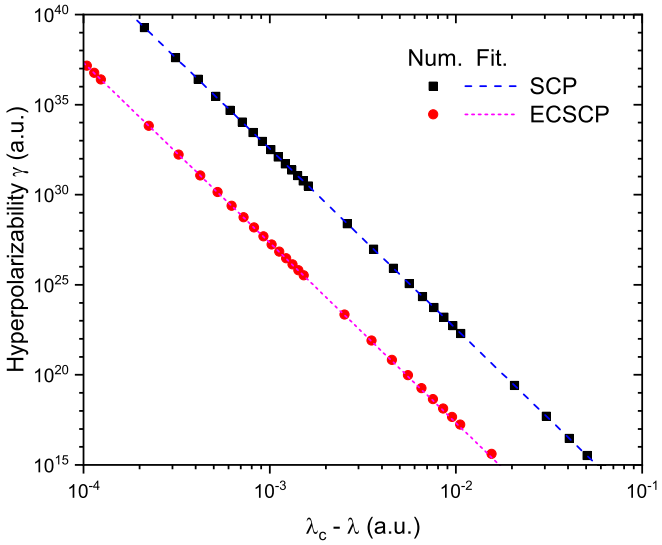

FIG. 3. Critical behavior of the hyperpolarizability for the ground state of H atom under SCP and ECSCP near corresponding critical screening parameters [$\lambda_c^{\mathrm{SCP}}(1s) = 1.190612421\ldots$ and $\lambda_c^{\mathrm{ECSCP}}(1s) = 0.720524085\ldots$]. Dots represent the present GPS numerical calculations and lines refer to the fittings based on the power function in Eq. (30).

However, due to the absence of approximate formulas for hyperpolarizability, even for the ground state of H-like atoms, we are currently unable to perform a similar analysis of the asymptotic behavior as we did in multipole polarizabilities. We present in Fig. 3 the numerical calculations and power-law fittings of the hyperpolarizabilities of the H atom in both SCP and ECSCP for screening parameters near the corresponding critical values. It is unambiguously observed that they both follow the tenth-order power law

$$\gamma(\lambda) \approx (\lambda_c - \lambda)^{-10}, \tag{30}$$

which means that the hyperpolarizability increases by six orders of magnitude faster than the dipole polarizability when the system approaches its continuum limit. Remembering that hyperpolarizability relates to the fourth-order energy correction in terms of the electric field strength, i.e., Eq. (11), it is expected that the perturbation series of system energy shown in Eq. (6) diverge faster as the field strength increases.

It is also interestingly found that Eqs. (27) and (30) show much similarity to, respectively, Eqs. (20) and (22) on the orders of the power laws. Their intrinsic connection is still unclear. Nevertheless, either formal analysis of the exact

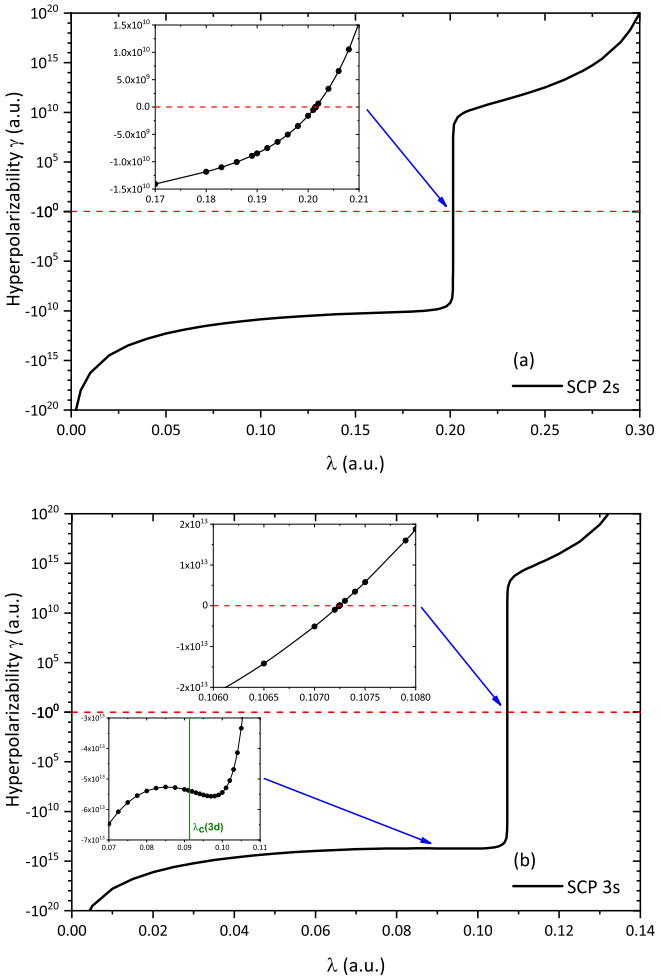

FIG. 4. Variation of the hyperpolarizability for the (a) $2s$ and (b) $3s$ excited states of H atom under SCP. The inset in (a) and the upper inset in (b) demonstrate the near-zero hyperpolarizabilities in the region of "tune-out" screening parameter. The lower inset in (b) indicates the contribution of the $3d$ state near its corresponding critical screening parameter [$\lambda_c^{\mathrm{SCP}}(3d) = 0.091345120\ldots$].

formula of hyperpolarizability or the development of new approximations would shed light on the asymptotic behavior of hyperpolarizability.

D. Excited states of the H atom under SCP and ECSCP

The static dipole hyperpolarizabilities for the $2s-5s$ excited states of the H atom under SCP and ECSCP are calculated by employing the same technique as that for the ground state, and their numerical values are provided in the Supplementary Material [45] for further reference.

In Figs. 4(a) and 4(b), the hyperpolarizabilities for the $2s$ and $3s$ states of the H atom under SCP are displayed to demonstrate the representative behavior of this quantity in excited states. It is interestingly found that, unlike in the ground state, the hyperpolarizability in excited states acquires an infinitely negative value at extremely small, but nonzero, screening parameters. This is nothing else but the sudden removal of the energy degeneracy in excited states with respect to the orbital angular momentum, e.g., $2s$ and $2p$ states

TABLE III. "Tune-out" screening parameters of hyperpolarizability for the $2s-5s$ excited states of H atom under SCP and ECSCP.

State	$\lambda_{\text{tune-out}}^{\text{SCP}}$	$\lambda_{\text{tune-out}}^{\text{ECSCP}}$
$2s$	0.201467610774525	0.143955330371167
$3s$	0.107245055195906	0.068263653379657
$4s$	0.065740732516004	0.039287893137210
$5s$	0.044177248516130	0.025439578475880

in the $n = 2$ shell and $3s$, $3p$, and $3d$ states in the $n = 3$ shell. It can be deduced from Eqs. (12) and (13) that, when λ increases slightly from zero, the extremely small energy difference in the denominator leads to infinitely large magnitudes of both polarizability and hyperpolarizability for the excited states. As the screening strength increases continuously, the hyperpolarizability increases smoothly, goes across zero, and finally approaches positive infinity at screening parameters near the corresponding critical value ($\lambda_c^{\mathrm{SCP}}(2s) = 0.310209282\ldots$ and $\lambda_c^{\mathrm{SCP}}(3s) = 0.139450294\ldots$). For the $3s$ excited state shown in Fig. 4(b), the hyperpolarizability shows an additional hump structure at about $\lambda = 0.09$. We identify this behavior as the contribution from the $3d$ state. Such a state transitions from a bound to continuum state exactly at $\lambda_c^{\mathrm{SCP}}(3d) = 0.091345120\ldots$, which would slightly suppress the increase of hyperpolarizability.

The zero value of hyperpolarizability attracts special interest in our research because, in this situation, the fourth-order energy correction disappears in the construction of the system's total energy, perturbed by the external electric field. We named these special screening parameters as "tune-out" screening parameters for hyperpolarizability, in a similar manner to the definition of tune-out wavelength for atomic dynamic dipole polarizability [46–48]. The tune-out screening parameters for the $2s-5s$ states of the H atom under SCP and ECSCP are listed in Table III and the determination of these parameters can be found in the Supplementary Material [45]. There exists only one tune-out screening parameter for each state and its magnitude decreases rapidly along with higher excited state. In the following section, we will show that the tune-out screening parameter is responsible for the cusp structure in the maximum effective field strength for excited states.

E. Applicability of hyperpolarizability

In this section, we would like to propose some empirical discussion on the range of application for the perturbation theory, or more precisely, the applicability of hyperpolarizability in estimating the energy of one-electron atoms in a plasma screening environment. As shown in Eq. (6), the perturbed series can only converge if the higher-order energy correction is smaller than the lower-order one. Because the hyperpolarizability is generally several orders of magnitude larger than the polarizability, we define a maximum effective electric field strength $F_{\max}$, where the fourth-order energy correction is equal to the second-order one, i.e.,

$$F_{\max}^2 E_k^{(2)} = F_{\max}^4 E_k^{(4)}. \tag{31}$$

TABLE IV. Maximum effective electric field strength $F_{\max}$ for the first five s-wave states of the free H atom. Numbers in parentheses represent powers of ten.

State	α	γ	$F_{\max}$
$1s$	4.5	1.333125(3)	2.0126184217(−1)
$2s$	1.2(2)	1.26432(7)	1.0672170182(−2)
$3s$	1.0125(3)	3.729453647625(9)	1.8049514809(−3)
$4s$	4.992(3)	2.48016273408(11)	4.9145959964(−4)
$5s$	1.78125(4)	6.996711181640625(12)	1.7478577648(−4)

Recalling Eqs. (10) and (11), we can establish that, in order to ensure the fourth-order energy correction to be smaller than the second-order term, the effective field strength must be in the range of

$$F < F_{\max} \equiv \sqrt{\frac{12\alpha}{|\gamma|}}, \tag{32}$$

where the absolute-value sign introduced in the denominator is attributed to the possible negative value of hyperpolarizability.

In Table IV, the estimated values of $F_{\max}$ for the free H atom (without plasma screenings) are displayed for the lowest five s-wave states. Both the polarizabilities and hyperpolarizabilities for these states are analytically available in the literature, so we conclude that the maximum effective electric field strengths shown in the table are accurate to the last reported digit. The fast decrease of the magnitude of $F_{\max}$ in higher-lying excited states indicates that the perturbation theory is more applicable for the ground state.

In the plasma screening environment, however, the situation differs intrinsically between the ground and excited states. In Fig. 5, our numerically calculated $F_{\max}$ for the ground state of H in SCP and ECSCP are displayed as a function of screening parameters. Due to the smooth increase of the hyperpolarizability from free H atom ($\lambda = 0$) to screened situations ($\lambda > 0$), as one can see from Table I, the value of $F_{\max}$ also decreases smoothly from 0.201261842... to zero as λ increases from zero to $\lambda_c^{\rm SCP}(1s)$ and $\lambda_c^{\rm ECSCP}(1s)$. The diminishing of $F_{\max}$ in stronger screening environments is simply due to the hyperpolarizability increasing faster than the polarizability. To be specific, as we discussed in Sec. III. C, the dipole polarizability increases by fourth power of $\lambda_c - \lambda$ in the asymptotic region, while the hyperpolarizability increases by tenth power.

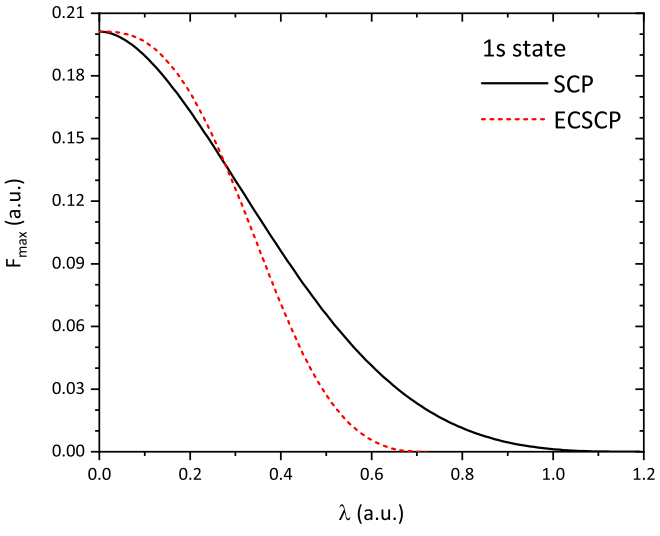

FIG. 5. Maximum effective electric-field strength for the ground state of H atom under SCP and ECSCP as a function of the screening parameter.

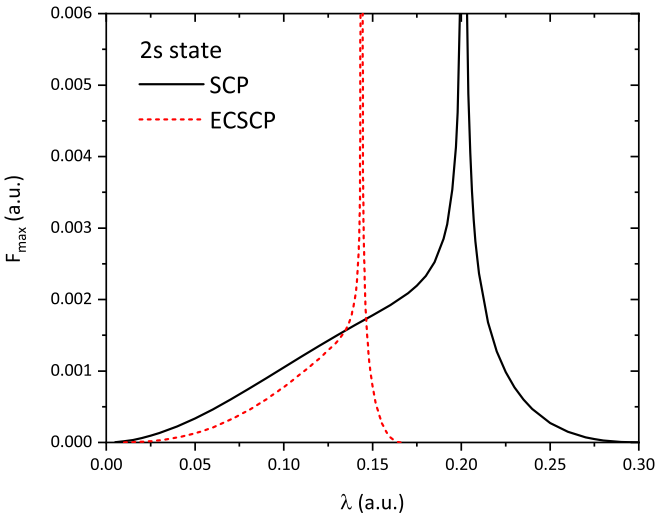

FIG. 6. Maximum effective electric field strength for the $2s$ state of H atom under SCP and ECSCP as a function of the screening parameter.

The variation of $F_{\max}$ for the $2s$ excited state shown in Fig. 6 reveals more interesting phenomena. It goes to zero in both the extreme situations of $\lambda \to 0$ and $\lambda \to \lambda_c^{\rm SCP(ECSCP)}(2s)$, which, respectively, are due to the negative and positive infinities of the hyperpolarizability in these two limits. In the middle of Fig. 6, a cusp structure appears exactly at the tune-out screening parameter $\lambda_{\text{tune-out}}^{\rm SCP(ECSCP)}(2s)$, where the hyperpolarizability incidentally reduces to zero (i.e., $F_{\max} = \infty$). The higher-lying excited states follow a similar trend and their variations are not discussed here for brevity. With great caution, we suggest that the application of hyperpolarizability in the excited states of one-electron atoms in a plasma screening environment needs further careful consideration.

Finally, it is of crucial importance to make quantitative comparisons between the perturbative estimations based on (hyper)polarizabilities and those nonperturbative calculations. There exist in the literature several sophisticated calculations of the ground-state energy of the H atom in the combination of plasma screening and electric field [49–53]. Essentially speaking, the spectra of the H atom in a static electric field are composed of resonance states (see Fig. 1 in Ref. [54]), no matter how small the field intensity is, and the system is more properly described in cylindrical or parabolic coordinates other than spherical coordinates. The complex-scaling (or complex-coordinate rotation) method [55] based on L^2-type basis functions was successfully employed to extract the resonance state energies and widths of the Debye-plasma screened H atom in a static electric field [50,52]. On the

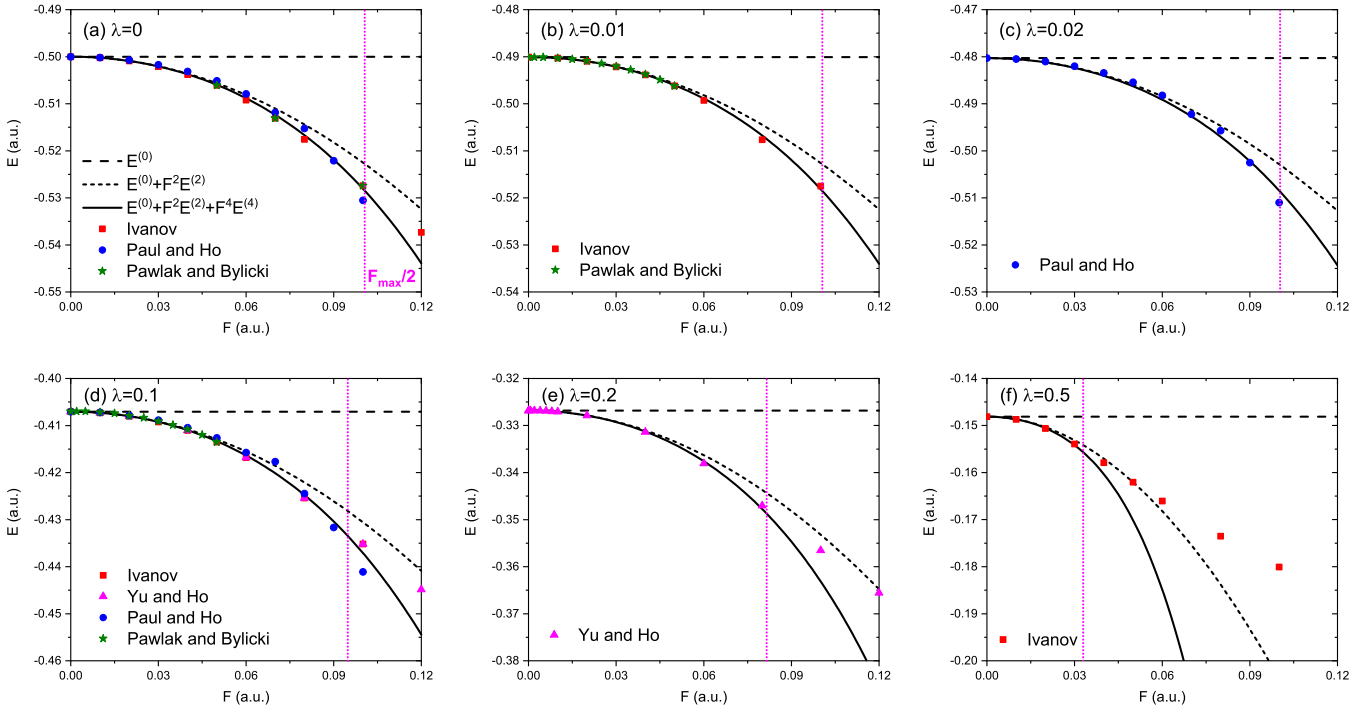

FIG. 7. Comparison of the zero-, second-, and fourth-order corrected energies for the ground state of H atom under SCP with previous nonperturbative calculations by Ivanov [49], Yu and Ho [50], Paul and Ho [51], and Pawlak and Bylicki [52]. (a) $\lambda = 0$, (b) $\lambda = 0.01$, (c) $\lambda = 0.02$, (d) $\lambda = 0.1$, (e) $\lambda = 0.2$, (f) $\lambda = 0.5$. In each figure, the vertical dotted line indicates the electric field strength of $F_{\max}/2$.

other hand, Paul and Ho [51] numerically verified that, when the electric field strength is relatively week, and so in this case the resonance width is much smaller than the associated resonance energy, the usual variational method can be safely used to estimate the system energy by treating the resonance state as a bound state. The perturbation treatment of this problem employed in the present work, i.e., Eqs. (6) and (7), although less accurate than the nonperturbative variational method, should also be applicable in the weak electric field.

In Fig. 7, we compare the present zero-order ($E^{(0)}$), second-order ($E^{(0)} + F^2E^{(2)}$), and fourth-order ($E^{(0)} + F^2E^{(2)} + F^4E^{(4)}$) corrected energies with those nonperturbative calculations for the ground state of the H atom in SCP at some selected values of the screening parameter. The zero-order energy depends only on the plasma screening parameter and, therefore, it does not change with respect to the field strength. The second-order effect due to polarizability lowers the ground-state energy, and the fourth-order correction due to hyperpolarizability reduces the energy further. For all screening parameters, the inclusion of fourth-order correction improves the agreement of perturbation estimation with the accurate complex-scaling and variational calculations in the weak-field region. However, it gradually underestimates the system energy in the strong-field region. In each figure, we empirically indicate the position of $F_{\max}/2$ [see Eq. (32) and Fig. 5 for the definition and variation of $F_{\max}$], smaller than which the fourth-order corrected energies are expected to reasonably reproduce the sophisticated calculations. From the comparisons shown in Fig. 7, we generally conclude that the applicability of hyperpolarizability, i.e., the fourth-order perturbation method, more likely lies in the range of $F \in [0, F_{\max}/2]$, in different plasma screening conditions.

For the H atom in ECSCP, to the best of our knowledge, the only complex-scaling calculation of the Stark resonances was performed by Wang *et al.* [56] recently. However, those authors primarily focused on high-lying resonance states and no numerical data or depicted figures for the ground state are available for comparison. In Fig. 8, the variation of the fourth-order corrected ground-state energy of the H atom with increasing electric field strength is displayed for

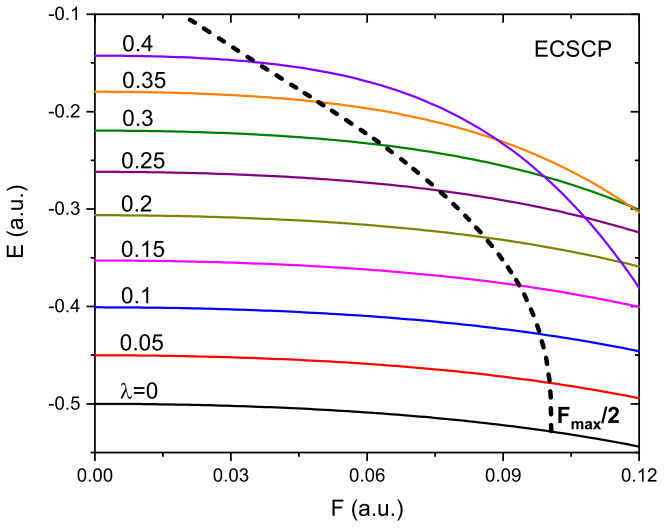

FIG. 8. The fourth-order corrected energies for the ground state of H atom under ECSCP at some selected values of screening parameter. The dotted line indicates the electric field strength of $F_{\max}/2$ beyond which the perturbation theory is expected to fail.

different screening parameters. The dividing line indicating the boundary at $F_{max}/2$, based on the same criteria in SCP, is also included to guide the eye. It is conjectured that the left region of the figure is responsible to predict the lowest resonance state energy of the H atom in ECSCP. Further sophisticated calculations based on complex-scaling or nonperturbative variational methods are necessary to elucidate such a conjecture.

IV. CONCLUSION

In this work, the hyperpolarizabilities of the H atom under Debye and dense quantum plasmas are investigated by employing the GPS method in the framework of sum-over-states formalism. The exponential convergence of the GPS method ensures that the present calculation provides a highly accurate prediction of hyperpolarizability, especially in the strong screening environment. When the system approaches the bound-continuum limit as the screening parameter gets close to the critical value, the hyperpolarizability increases by a tenth-power law, which is six orders of magnitude larger than that for the dipole polarizability.

We further extended the calculation to the excited states of the H atom in both of two model plasmas. It is interestingly found that when the screening effect is just introduced into the system, the hyperpolarizability jumps from the free-atom finite value to negative infinity, which is due to the sudden removal of the energy degeneracy with respect to the orbital angular momentum. With continuously increasing the screening strength, the hyperpolarizability goes across zero at the so-called "tune-out" screening parameter, and finally follows the asymptotic behavior near corresponding critical screening parameters. Such a different trend between the excited and ground states implies a divergent behavior of the maximum field strength F_{max}, which is defined by equating the second- and fourth-order energy corrections.

We finally focus on the applicability of hyperpolarizability in estimating the ground-state energy of the H atom in a plasma screening environment. By comparing the fourth-order corrected energies for H atom in Debye plasmas with those nonperturbative complex-scaling and variational calculations existing in the literature, we empirically conclude that the effective electric-field strength lies in the range of $[0, F_{max}/2]$, so that the perturbative calculations based on (hyper)polarizabilities can reasonably reproduce the physical resonance state energies. The confirmation of such a conjecture for the H atom in dense quantum plasmas still needs further verification by complex-scaling calculations.

The data that support the findings of this study are available within the article.

ACKNOWLEDGMENT

Financial support from the National Natural Science Foundation of China (Grants No. 12174147 and No. 11774131) is greatly acknowledged.

[1] J. C. Weisheit and M. S. Murillo, *Springer Handbook of Atomic, Molecular, and Optical Physics*, edited by G. W. F. Drake, (Springer, New York, 2006), Chap. 86, p. 1303.
[2] B. Saha, P. K. Mukherjee, and G. H. F. Diercksen, Astron. Astrophys. **396**, 337 (2002).
[3] B. Saha and S. Fritzsche, Phys. Rev. E **73**, 036405 (2006).
[4] A. N. Sil, S. Canuto, and P. K. Mukherjee, Adv. Quantum Chem. **58**, 115 (2009).
[5] S. B. Zhang, J. G. Wang, and R. K. Janev, Phys. Rev. Lett. **104**, 023203 (2010).
[6] R. K. Janev, S. B. Zhang, and J. G. Wang, Matter Radiat. Extremes **1**, 237 (2016).
[7] J. Deprince, M. A. Bautista, S. Fritzsche, J. A. García, T. R. Kallman, C. Mendoza, P. Palmeri, and P. Quinet, Astron. Astrophys. **624**, A74 (2019).
[8] P. Palmeri, J. Deprince, M. A. Bautista, S. Fritzsche, J. A. García, T. R. Kallman, C. Mendoza, and P. Quinet, Astron. Astrophys. **657**, A61 (2022).
[9] J. K. Saha, T. K. Mukherjee, P. K. Mukherjee, and B. Fricke, Eur. Phys. J. D **62**, 205 (2011).
[10] S. Bhattacharyya, P. K. Mukherjee, and B. Fricke, Phys. Lett. A **384**, 126115 (2020).
[11] S. Bhattacharyya, P. K. Mukherjee, and B. Fricke, Int. J. Quantum Chem. **120**, e26422 (2020).
[12] S. K. Chaudhuri, S. Bhattacharyya, R. K. Chaudhuri, and P. K. Mukherjee, Phys. Lett. A **402**, 127343 (2021).
[13] S. Sen, P. Mandal, and P. K. Mukherjee, Phys. Plasmas **19**, 033501 (2012).
[14] S. Sen, P. Mandal, P. K. Mukherjee, and B. Fricke, Phys. Plasmas **20**, 013505 (2013).
[15] S. K. Chaudhuri, P. K. Mukherjee, and B. Fricke, Phys. Plasmas **22**, 123120 (2015).
[16] S. Kang, J. He, N. Xu, and C. Y. Chen, Commun. Theor. Phys. **62**, 881 (2014).
[17] D. P. Shelton, Phys. Rev. A **36**, 3032 (1987).
[18] D. M. Bishop, Theor. Comput. Chem. **6**, 129 (1999).
[19] G. L. Sewell, Math. Proc. Camb. Philos. Soc. **45**, 678 (1949).
[20] D. M. Bishop and J. Pipin, Chem. Phys. Lett. **236**, 15 (1995).
[21] M.-A. Martínez-Sánchez, C. Martínez-Flores, R. Vargas, J. Garza, R. Cabrera-Trujillo, and K. D. Sen, Phys. Rev. E **103**, 043202 (2021).
[22] P. Debye and E. Hückel, Z. Phys. **24**, 185 (1923).
[23] P. K. Shukla and B. Eliasson, Phys. Lett. A **372**, 2897 (2008).
[24] P. K. Shukla and B. Eliasson, Rev. Mod. Phys. **83**, 885 (2011).
[25] P. K. Shukla and B. Eliasson, Phys. Rev. Lett. **108**, 165007 (2012).
[26] L. G. Jiao, Y. Y. He, Y. Z. Zhang, and Y. K. Ho, J. Phys. B: At. Mol. Opt. Phys. **54**, 065005 (2021).
[27] G. Yao and S. I. Chu, Chem. Phys. Lett. **204**, 381 (1993).
[28] S. I. Chu and D. A. Telnov, Phys. Rep. **390**, 1 (2004).
[29] L. Zhu, Y. Y. He, L. G. Jiao, Y. C. Wang, and Y. K. Ho, Int. J. Quantum Chem. **120**, e26245 (2020).
[30] D. J. Griffiths, *Introduction to Quantum Mechanics* (Pearson Education International, Hoboken, NJ, 2005).
[31] L. L. Boyle, A. D. Buckingham, R. L. Disch, and D. A. Dunmur, J. Chem. Phys. **45**, 1318 (1966).

[32] C. Canuto, M. Y. Hussaini, A. Quarteroni, and T. A. Zang, *Spectral Methods: Fundamentals in Single Domains* (Springer, Berlin, 2006).
[33] L. Zhu, Y. Y. He, L. G. Jiao, Y. C. Wang, and Y. K. Ho, Phys. Plasmas **27**, 072101 (2020).
[34] C. G. Diaz, F. M. Fernández, and E. A. Castro, J. Phys. A: Math. Gen. **24**, 2061 (1991).
[35] L. G. Jiao, H. H. Xie, A. Liu, H. E. Montgomery, Jr., and Y. K. Ho, J. Phys. B: At. Mol. Opt. Phys. **54**, 175002 (2021).
[36] A. K. Bhatia and R. J. Drachman, Atoms **9**, 86 (2021).
[37] R. J. Drachman and A. K. Bhatia, Phys. Rev. A **51**, 2926 (1995).
[38] Y. Y. He, L. G. Jiao, A. Liu, Y. Z. Zhang, and Y. K. Ho, Eur. Phys. J. D **75**, 126 (2021).
[39] X. R. Wang, Phys. Rev. A **46**, 7295 (1992).
[40] J. G. Kirkwood, Z. Phys. **33**, 57 (1932).
[41] R. A. Buckingham, Proc. Roy. Soc. A **160**, 94 (1937).
[42] A. Unsöld, Z. Phys. **43**, 563 (1927).
[43] A. Dalgarno and J. T. Lewis, Proc. Roy. Soc. Lond. A **240**, 284 (1957).
[44] V. I. Pupyshev and H. E. Montgomery, Jr., Int. J. Quantum Chem. **119**, e25887 (2019).
[45] See Supplemental Material at http://link.aps.org/supplemental/10.1103/PhysRevE.107.045201 for a complete list of hyperpolarizabilities for the $2s-5s$ states of the H atom in Debye and dense quantum plasmas.
[46] L. J. LeBlanc and J. H. Thywissen, Phys. Rev. A **75**, 053612 (2007).
[47] B. Arora, M. S. Safronova, and C. W. Clark, Phys. Rev. A **84**, 043401 (2011).
[48] S. Kar, Y.-S. Wang, Z. Jiang, Y. Wang, and Y. K. Ho, Chinese J. Phys. **56**, 3085 (2018).
[49] M. V. Ivanov, J. Phys. B: At. Mol. Opt. Phys. **34**, 2447 (2001).
[50] A. C. H. Yu and Y. K. Ho, Phys. Plasmas **12**, 043302 (2005).
[51] S. Paul and Y. K. Ho, Phys. Plasmas **17**, 082704 (2010).
[52] M. Pawlak and M. Bylicki, Phys. Rev. A **83**, 023419 (2011).
[53] C. Y. Lin and Y. K. Ho, J. Phys. B: At. Mol. Opt. Phys. **44**, 175001 (2011).
[54] L. Fernández-Menchero and H. P. Summers, Phys. Rev. A **88**, 022509 (2013).
[55] Y. K. Ho, Phys. Rep. **99**, 1 (1983).
[56] X.-W. Wang, S.-W. Chen, and J.-Y. Guo, J. Phys. B: At. Mol. Opt. Phys. **52**, 025001 (2019).